

Novel pyrazole derivatives as inhibitors of stainless steel in 2.0M H₂SO₄ media: Electrochemical Study

Hoyam Chahmout ¹, Moussa Ouakki ^{1,*}, Sarra Sibous ², Mouhsine Galai ³, Zakaria Benzekri ², Saïd Boukhris ², Abdelaziz Souizi ² and Mohammed Cherkaoui ^{1,4}

¹Laboratory of materials, electrochemistry and environment, Faculty of Science, Ibn Tofail University, PB 133-14050 Kénitra, Morocco

²Laboratory of chimie organique, organométallique and théorique, Faculty of Science, Ibn Tofail University, PB 133-14050 Kénitra, Morocco

³Laboratory of Materials Engineering and Environment: Modeling and Application, Faculty of Science, Ibn Tofail University, PB 133-14050 Kénitra, Morocco

⁴National Higher School of Chemistry, Ibn Tofail University, PB 133-14050 Kénitra, Morocco

Abstract: Metallic materials are well known and widely used in various industrial sectors. However, they can be easily corroded in various aggressive environments. The protective action of stainless steel by two organic pyrazole compounds: {1-amino-5,10-dioxo-3-(p-tolyl)-5,10-dihydro-1H-pyrazolo[1,2-b]phthalazine-2-carbonitrile} and {1-amino-3-(2-chlorophenyl)-5,10-dioxo-5,10-dihydro-1H-pyrazolo[1,2-b] phthalazine-2-carbonitrile} in H₂SO₄ 2.0M medium was studied using the electrochemical technics (Electrochemical Impedance Spectroscopy (EIS), potentiodynamic polarization), Scanning Electron Microscopy (SEM) and Energy Dispersion X-ray spectroscopy (EDX). Polarization curves indicate that both compounds act as anodic inhibitors. A suitable equivalent electrical circuit model was used to calculate the impedance parameters. The adsorption study showed that these compounds are adsorbed to the steel surface according to the adsorption isotherm of Langmuir. Effect of temperature was also investigated and activation parameters were evaluated.

Keywords: Corrosion inhibition; Pyrazole derivatives; EIS; H₂SO₄; SEM/EDX.

1. Introduction

Stainless steel is widely used in different sectors of industry: chemical ¹⁻³, food industry ^{4,5}, pharmaceutical, petrochemical ⁶, heat exchangers, reservoirs, and structural materials ⁷... because of their excellent mechanical properties ⁸, their ease of manufacture, their relatively low cost especially for implantable medical devices and their reasonable resistance to corrosion. Among all these properties, corrosion resistance of stainless steel has attracted our attention.

Stainless steels are capable of forming passive layers on the surface, giving the material an excellent corrosion resistance. But the use of aggressive agents, usually acid solutions in the industry of cleaning, pickling, descaling and acidification of oil wells ⁹⁻¹¹, destroys this passivation, thus making the surface-active. Various corrosion protection methods are used to reduce its attack on metallic materials.

Several methods of corrosion protection have been considered so far by several authors ^{12,13}. These methods can be classified between those that modify

the potential of the electrode on the metal surface or those that modify the nature of the metal itself. Cathodic protection and anodic protection are two methods of corrosion control by changing the electrode potential ^{14,15}.

The nature of the metal can be modified by the use of metal coatings (sacrificial or noble) or by the choice of a material from which a more corrosion-resistant alloy is selected rather than a less corrosion-resistant alloy. However, most frequently, the choice of materials is not an option because of the need to maintain other desirable properties (such as mechanical strength) or is prohibited by cost. In such cases, the modification of the environment by the use of corrosion inhibitors becomes a possible means of corrosion control ¹⁶. However, the use of corrosion inhibitors has been found to be the most effective and the cheapest method for protection and prevention of steel ¹⁷. Current researches are increasingly moving towards the use of non-toxic ¹⁸⁻²¹ and stable organic molecules to inhibitor reduce corrosion.

*Corresponding author: Moussa Ouakki

Email address: moussassaw@gmail.com

DOI: <http://dx.doi.org/10.13171/mjc02003161235mo>

Received December 22, 2020

Accepted January 28, 2020

Published March 16, 2020

The inhibitory action of these organic compounds, which is generally independent of anodic and cathodic corrosion processes, is related to the formation by adsorption of a more or less continuous but finite thickness barrier, which prevents the solution from accessing the metal. The most efficient and effective corrosion inhibitors are organic compounds containing electronegative functional groups, π -electrons, in conjugated double or triple bonds or aromatic rings. There is also a specific interaction between functional groups containing hetero atoms like nitrogen, sulfur, oxygen, having free lone pair of electrons and the metal surface, which play an essential role in inhibition. When two of these features are combined, increased inhibition can be observed^{22,23}. Recently many researchers have reoriented their attention to the use of new organic compounds as corrosion inhibitors such as pyrazole^{24,25}, triazole^{26,27}, tetrazole^{28,29}, pyrazole^{30,31} and imidazole^{32,33}. Recently, pyrazole has attracted a lot of attention in the field of metallic corrosion inhibition due to their attractive properties, the choice of these compounds is based on molecular structure considerations, i.e., the number of active centers and type of substituents present in these compounds.

Most organic compounds inhibit corrosion via adsorption on the metal surface. This adsorption mainly depends on some physicochemical properties of the molecule, related to its functional groups (e.g. nitrogen, oxygen and sulfur atoms), aromaticity, the possible steric effects and electronic density. This work aims to study the inhibition properties of two pyrazole derivatives³⁴ on stainless steel corrosion in 2.0 M H_2SO_4 using potentiodynamic polarization curves, and electrochemical impedance spectroscopy. It also aims to predict the thermodynamic feasibility of these compounds on the steel surface. Also, a detailed investigation of temperature was also carried and discussed to improve a better understanding of the adsorption mechanism of the studied inhibitors.

2. Experimental conditions

2.1. Material and medium

The corrosive medium is a sulfuric acid solution H_2SO_4 with a concentration of 2.0M, obtained by diluting 98% concentrated commercial acid with distilled water.

The tested material is stainless steel. The weight content composition of the basic elements of stainless steel is given in Table 1.

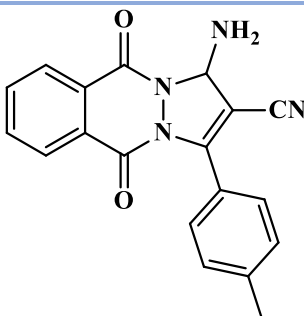
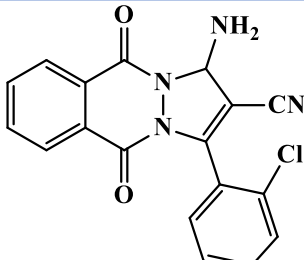
Table 1. Chemical composition of stainless steel (% wt).

Elements	Fe	C	Si	Mn	P	S	N	Cr	Co	Mo	Ni	Cu
% wt	Bal	0,04	0,41	1,46	0,07	0,03	0,08	18,5	0,16	0,33	7,81	0,51

The steel sample is in the form of a plate, having a surface of the order of 1cm^2 in contact with the electrolyte.

In order to obtain reliable and reproducible results, the stainless-steel samples are prepared before each test by polishing with an abrasive paper of increasing size (grade 200 to 2000), rinsed with distilled water and finally dried.

Table 2. Structures and Nomenclature of the pyrazole molecules studied.

Abbreviation	Chemical structure	IUPAC Name / molecular formula / Molar mass
P1		1-amino-5,10-dioxo-3-(p-tolyl)-5,10-dihydro-1H-pyrazolo[1,2-b]phthalazine-2-carbonitrile $C_{19}H_{14}N_4O_2$ 330,34 g/mol
P2		1-amino-3-(2-chlorophenyl)-5,10-dioxo-5,10-dihydro-1H-pyrazolo[1,2-b]phthalazine-2-carbonitrile $C_{18}H_{11}N_4O_2Cl$ 350,759 g/mol

We will examine the influence of the addition of 10^{-6}M to 10^{-3}M of the two organic products based on pyrazole on the inhibition of corrosion of stainless steel in acidic medium H_2SO_4 2.0M. The molecular structures of those compounds are illustrated in Table 2.

2.2. Electrochemical study techniques

Electrochemical methods can be classified into two techniques: stationary methods and transient methods. From a phenomenological point of view, the characterization of the compound's adsorption is possible by the monitoring of the open-circuit potential. This measurement gives a characterization of the modification of the metal/medium interface. The more quantitative aspect (polarization curves, electrochemical impedance spectroscopy) provides access to values of the physical parameters describing the state of the system (corrosion current, inhibition rate, double layer capacity, charge transfer resistance, ...) ³⁵.

2.2.1. Stationary methods

The electrochemical study of the behaviour of stainless steel towards the corrosive environment in the absence or in the presence of organic compounds is based mainly on the plots of the polarization curves using an experimental device consisting of a Potentiostat-Galvanostat PGZ 100, a microcomputer with software «Voltmaster4».

Corrosion inhibition efficiency η_{pp} is defined by the following expression (1):

$$\eta_{pp} \% = \left[\frac{(i_{corr}^{\circ} - i_{corr})}{i_{corr}^{\circ}} \right] \cdot 100 \quad (1)$$

Where i_{corr}° and i_{corr} are the corrosion current densities in the absence and in the presence of inhibitor, respectively.

The equilibrium potential of this study is measured after 30 minutes of the sample immersion in the acid medium in the absence and in the presence of both products.

The polarization curve has been plotted in a potential domain corresponding to (-900 mV/Ag/AgCl to 400mV/Ag/AgCl) with a scan rate of 1mV/s. In the drawing of the Tafel lines, we consider only the field of linearity of the cathodic and anodic branches which are limited for this experiment to ± 100 mV on either side of the corrosion potential.

These stationary techniques, however, remain insufficient to characterize complex mechanisms, involving several reactive steps and having different

characteristic kinetics (which is the case during inhibition processes). The use of transient techniques then becomes essential ³⁶.

2.2.2. Transient methods

Transient techniques are based on the disturbance of the physical quantities of the electrochemical system so that the system response can be analyzed in a time-invariant linear domain.

Electrochemical impedance spectroscopy is a non-stationary method that provides information on the elementary steps that make up the overall electrochemical process. Its principle is to superimpose a low-amplitude sinusoidal potential modulation on the electrode's potential and to track the current response for different frequencies of the disruptive signal. The current response is also sinusoidal, superimposed on the current stationary but out of the phase at an angle θ to the potential. Conversely, a current can be imposed and the potential recorded ³⁷.

Impedance measurements are made at 298K after half an hour of immersion in an acid medium. The amplitude of the line voltage applied to the abandonment potential is 10 mV peak-to-peak, at frequencies between 100 kHz and 10 MHz, with 10 measurement points per decade with open circuit potential.

The corrosion inhibition efficiency of the steel is calculated from the polarization resistance, according to (2):

$$\eta_{imp} \% = (R_p - R_p^{\circ} / R_p) \cdot 100 ; \theta = R_p - R_p^{\circ} / R_p \quad (2)$$

Where R_p° and R_p are the polarization resistances in the absence and in the presence of inhibitor, respectively, θ is the recovery rate.

2.3. Surface characterization by SEM/EDX

The determination of the nature of the film formed on the surface of the metal exposed to H_2SO_4 2.0M solution for 6h in the absence and in the presence of the inhibitors studied was carried out by the scanning electron microscope observation of type Quanta FEG 450 coupled with EDX analyses. Those analyses were realized in MAScIR-Rabat foundation.

3. Results and discussion

3.1. Stationary electrochemical study

Figure 1 presents the anodic and cathodic polarization curves for stainless steel in H_2SO_4 2.0M medium, in the absence and in the presence of P1 and P2 at different concentrations and 298K.

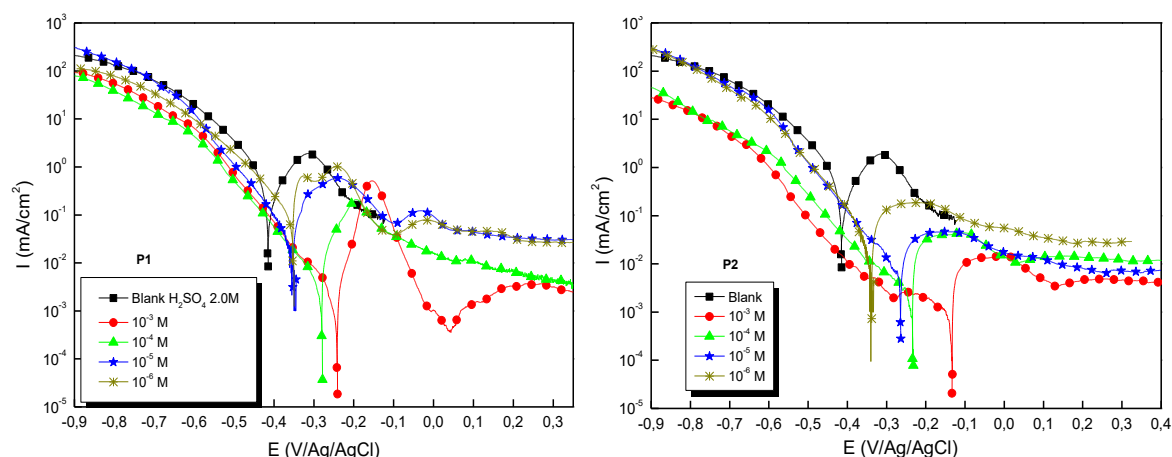


Figure 1. Representation of the anodic and cathodic polarization curves for stainless steel in H_2SO_4 2.0M medium, in the absence and in the presence of P1 and P2 at different concentrations and 298K

An initial analysis of these curves shows that the anodic and cathodic reactions are affected by the addition of the P1 and P2 compounds. The addition of the inhibitor in H_2SO_4 2.0M solution significantly retarded both cathodic (hydrogen evolution) and anodic reactions (stainless dissolution). This behaviour reflects the inhibitory action of both products³⁸. Moreover, the polarization curves shifted toward lower corrosion current densities (i_{corr}) and less negative corrosion potentials (E_{corr}) in the presence of the tested compounds. The displacement of the curves was more pronounced in the anodic curves, which corresponds to the dominant anodic inhibition mechanism of the pyrazole derivatives. However, the corrosion potential showed a significant

change in the presence of the pyrazole derivatives. Therefore, the two compounds can be classified as anodic type inhibitor³⁹. According to Figure 1, the cathodic branches followed typical Tafel behavior throughout a wide range of current and potential which means that cathodic slopes could be calculated accurately. On the other hand, no linear Tafel region was observed on the anodic branches of the curves. Consequently, the values of anodic Tafel slopes (β_a).

Table 3 shows the values of the electrochemical parameters determined from the polarization curves previously obtained: corrosion current density (i_{corr}), corrosion potential (E_{corr}), cathodic Tafel slopes (β_c) as well as the corrosion inhibitor efficiency $\eta_{\text{PP}}(\%)$.

Table 3. Inhibition efficiency and electrochemical parameters determined from the polarization curves of stainless steel in H_2SO_4 2.0M without and with the addition of P1 and P2.

Medium	Conc. M	$-E_{\text{corr}}$ mV/Ag/AgCl	i_{corr} $\mu\text{A cm}^{-2}$	$-\beta_c$ mV dec ⁻¹	η_{PP} %
H_2SO_4 2.0 M	--	412	827	135	--
P1	10^{-6}	337	344,8	112	58,3
	10^{-5}	347	282,8	104	65,8
	10^{-4}	278	82,5	100	90,0
	10^{-3}	248	57,5	110	93,0
P2	10^{-6}	329	359	126	56,6
	10^{-5}	265	129	114	84,4
	10^{-4}	232	22	129	97,3
	10^{-3}	133	13	124	98,4

The analysis in Table 3 shows a significant decrease in the corrosion current density (i_{corr}) as the concentration of the tested products increases involving an improvement in inhibitor efficiency.

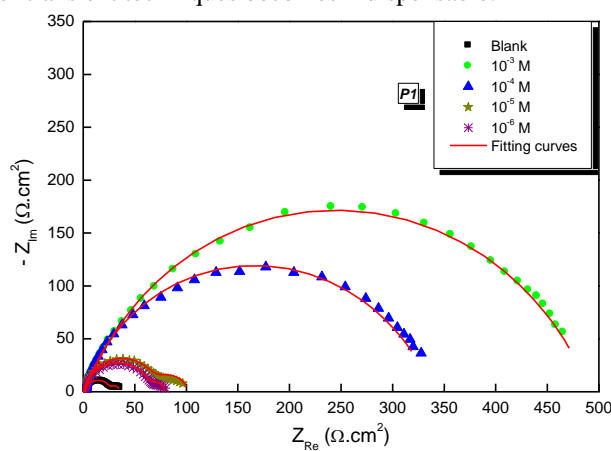
In the presence of inhibitors, the corrosion potential E_{corr} moves towards more anodic values. In literature, it has been reported that if the absolute corrosion potential displacement E_{corr} (inhibitor) is > 85 mV

compared to the blank E_{corr} , the inhibitor can be classified as anodic or cathodic, and if the movement in E_{corr} is < 85 mV, the inhibitor can be considered as mixed type⁴⁰. In our study, the maximum displacement of the corrosion potential E_{corr} was more than 85 mV, indicating that P1 and P2 act as anodic type inhibitors.

The compound P2 is therefore classified as the best with maximum inhibition efficiency of 98.4% for a concentration of 10^{-3} M, in agreement with the lowest corrosion current density value of $13\mu\text{A}/\text{cm}^2$.

This excellent efficiency is explained by the presence of high electronic densities on the molecules due to the existence of the nonbinding doublets of the heteroatoms (N and O) and electrons (π) of the aromaticity, which favors the adsorption process on the metal⁴¹⁻⁴⁴.

This stationary electrochemical technique, however, remains very limited in characterizing complex mechanisms, involving several reactive steps and having different characteristic kinetics. Thus, the use of transient techniques becomes indispensable.



3.2. Transient electrochemical study

To fully understand the mechanism of the process taking place at the electrode/solution interface, the electrochemical impedance measurements were carried out. This technique makes it possible to differentiate reaction processes by their relaxation time.

The results of this method are given as impedance diagrams in the Nyquist (Figure 2) and Bode planes (Figure 4). Impedance diagrams of the stainless steel immersed in the H_2SO_4 2.0M corrosive solutions without and with the addition of the inhibitor P1 and P2 at different concentrations are shown in Figure 2

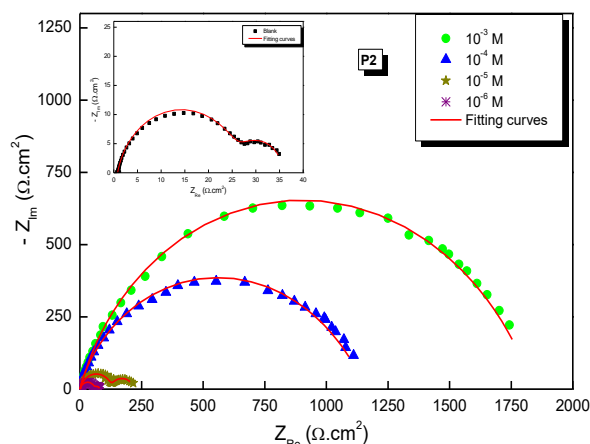


Figure 2. Nyquist plots of stainless steel in H_2SO_4 2.0M medium without and with different concentrations of P1 and P2

The Nyquist plots are characterized by two capacitive loops: one at high frequency attributed to the presence of the film, and the second at low frequency attributed to the charge transfer resistance. It is also observed that the size of the loop increases progressively with the addition of different concentrations of the tested inhibitors⁴⁵. This result reflects the influence of the inhibitor on the corrosion process at the steel interface in H_2SO_4 2.0M as explained in stationary studies.

The Nyquist impedance spectra of stainless steel in H_2SO_4 2.0M were simulated by the equivalent circuit

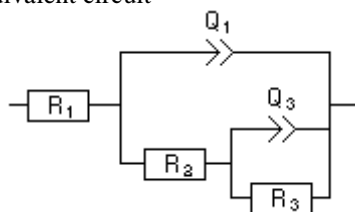


Figure 3. The equivalent circuit used to simulate the impedance spectra

Where $R_1=R_s$, $Q_1=Q_f$, $R_2=R_f$, $Q_3=Q_{dl}$ and $R_3=R_{ct}$.

As can be seen in Figure 3, the capacitor was changed by a constant phase element, indicating the presence of dissimilar frequency response. CPE impedance is defined as follows (3)^{47,48}:

$$Z_{CPE}(\omega) = Q^{-1}(j\omega)^{-1} \quad (3)$$

shown in Figure 3. The following elements are the components of the suggested equivalent circuit: R_s presents the solution resistance, R_{ct} charge transfer resistance, R_f the film resistance, and Q_f and Q_{dl} are the elements with constant phase⁴⁶.

The equivalent circuit analyzed all impedance spectra obtained from the steel electrode exposed for 30 min in H_2SO_4 2M solutions containing P1 and P2 in Figure 3.

With Q : a constant whose unity is $\Omega \cdot \text{cm}^{-2} \cdot \text{s}^n$, ω : Angular frequency in rad s^{-1} , n is the CPE exponent with $-1 < n < 1$. Z_{CPE} can represent an inductance ($n = -1$), a Warburg impedance ($n = 0.5$), a pure capacity ($n = 1$), or a resistance ($n = 0$). The smaller the n value, the higher the surface roughness⁴⁹⁻⁵¹.

Electrochemical parameters obtained from impedance diagrams and inhibitor efficiency (E%) are grouped in Table 4. The polarization resistance R_p values of all systems are calculated using the following equation:

$$R_p = R_f + R_{ct}$$

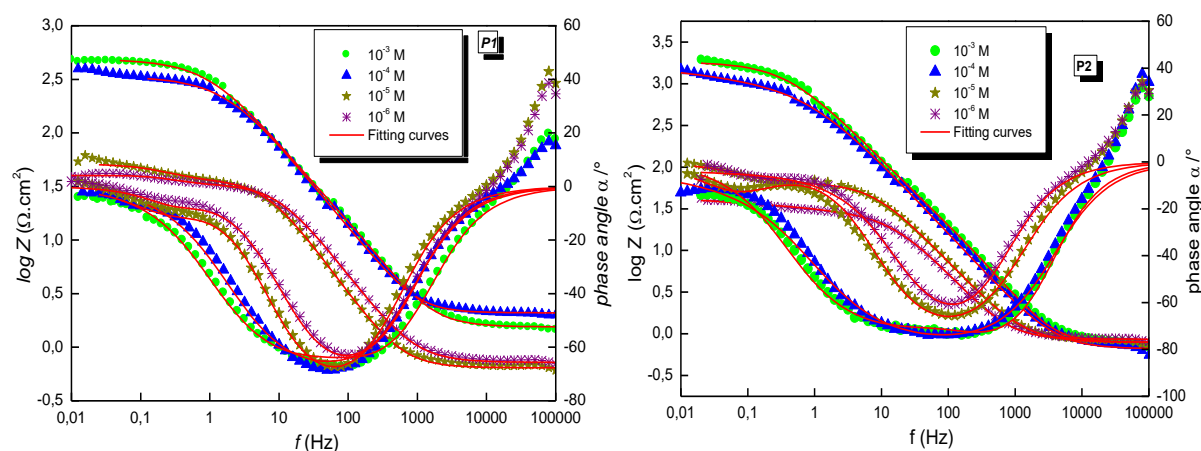


Figure 4. Bode spectrum of steel in H_2SO_4 2.0M solution in the absence and the presence of P1 and P2 at different concentrations

Bode spectrum obtained for steel in the absence and in the presence of P1 and P2 (Figure 4) shows two maximum phases at intermediate and low frequencies.

The Bode Representation confirms the use of two electrical circuits to simulate experimental data.

Table 4. Inhibition efficiency and electrochemical parameters determined from the electrochemical impedance measurements of stainless steel in H_2SO_4 2.0M without and with the addition of the inhibitor.

Inhibitors	Con M	R_s $\Omega.cm^2$	Q_f $\mu F.S^{n-1}$	n_f	R_f $\Omega.cm^2$	Q_{ct} $\mu F.S^{n-1}$	n_{ct}	R_{ct} $\Omega.cm^2$	R_p $\Omega.cm^2$	E%	θ
H_2SO_4 2.0 M	--	0,8	958	0,864	26,8	625	1	8,1	34,9	--	--
P1	10^{-6}	0,7	673	0,875	66,4	433	0,984	15,0	81,4	57,1	0,571
	10^{-5}	0,6	511	0,910	72,0	406	0,858	29,4	101,4	65,6	0,656
	10^{-4}	2,0	162	0,934	23,0	391	0,664	315,3	338,3	89,7	0,897
	10^{-3}	1,5	185	0,895	37,3	356	0,696	453,2	490,5	92,9	0,929
P2	10^{-6}	0,9	698,7	0,878	57,2	613	0,729	23,0	80,2	56,5	0,565
	10^{-5}	0,8	522,3	0,865	128,8	576	0,844	88,2	217	83,9	0,839
	10^{-4}	0,6	60,6	0,999	40,7	341	0,688	1155	1195,7	97,1	0,971
	10^{-3}	0,7	90,8	0,950	40,5	216	0,706	1803	1843,5	98,1	0,981

From the data in Table 4, it can be seen that as these compounds concentrations increase, R_p values increase, while the Q_f values decrease. These evolutions indicate thickening of the film formed and a decrease in permeability through it⁵². Consequently, the decrease in Q_f values shows that the adsorption layer formed by this compounds on the metal surface is stable⁵³. The decrease in Q_f may result from a local decrease in dielectric constant and/or an increase in double-layer thickness; this was attributed to the gradual replacement of water molecules and other ions initially adsorbed on the surface by adsorption of inhibitor molecules on the metal surface⁵⁴⁻⁵⁶. According to the Helmholtz model, the capacity of the

double layer C_{dl} is given by the following equation (4)^{57,58}:

$$C_{dc} = \epsilon \epsilon_0 S / e \quad (4)$$

Where e is the deposit thickness, ϵ is the dielectric constant, ϵ_0 is the Permittivity of the medium ($8.854 \times 10^{-14} F cm^{-1}$) and S the electrode surface.

The inhibitory efficiency (E%) increases with increasing inhibitor concentrations which is related to an increase in R_p values, indicating better adsorption of the inhibitor molecules on the steel surface. These conventional results have been fully explained by many authors^{18, 59}.

Inhibition efficiencies calculated from EIS show the same trend as those estimated from polarization measurements.

3.3. Adsorption isotherm

An adsorption study was performed to explain the inhibition effect of organic molecules on the corrosion of steel. This effect is described by two main types of adsorption: physical adsorption and chemical adsorption. It depends on the charge of the metal, its nature, the chemical structure of the organic product and the type of electrolyte.

In an aqueous solution, the adsorption of organic molecules from the solution to the metal interface is usually accompanied by the desorption of water molecules already adsorbed on the metal surface. This adsorption is therefore regarded as a phenomenon of substitutional adsorption, as the following reaction shows (5):

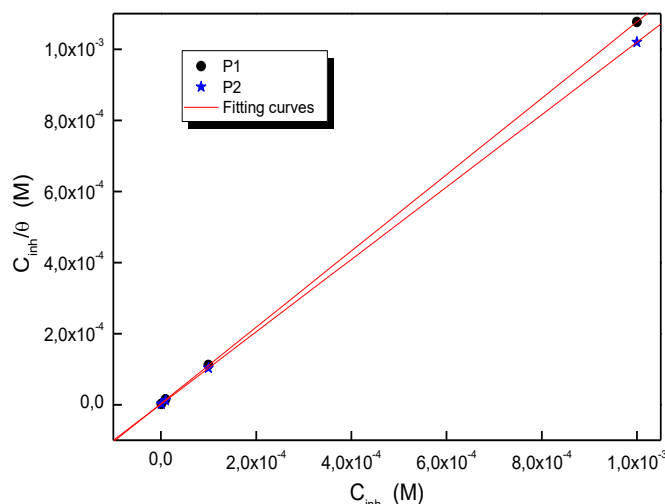
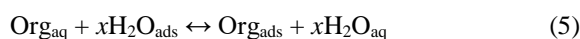


Fig. 5 The adsorption isotherm of Langmuir for P1 and P2 on the stainless-steel surface at 298 K

The best description of the adsorption behavior of studied inhibitors was explained by Langmuir adsorption isotherm (Figure 5)⁶¹, as the average linear regression coefficient values (R^2) obtained for P1 and P2 and slope are very close to unity.

The value of K_{ads} was found to be large, namely, $325.97 \cdot 10^3$ (L/mol) of P1 and $819.39 \cdot 10^3$ (L/mol) of P2, implying efficient adsorption, this can be explained simply by the presence of several donor

x is the number of water molecules replaced by the inhibitor molecule.

Several types of adsorption isotherms are present to assess the adsorption phenomenon on the metal surface (for example, the Langmuir isotherm, Temkin, Frumkin, etc.³³). The experimental values obtained from EIS are studied for the adjustment of several types of adsorption isotherms. Among the isotherms, the adsorption isotherm of Langmuir shows a fine adjustment of the experimental values. The Langmuir isotherm determined by the metal surface coverage ratio (Θ) is related to the inhibitor concentration by the relationship (6)⁶⁰:

$$\frac{C_{\text{inh}}}{\theta} = \frac{1}{K_{\text{ads}}} + C_{\text{inh}} \quad (6)$$

Where K_{ads} the equilibrium constant of the adsorption process and C_{inh} the inhibitor concentration in the solution. The variation of the ratio C_{inh}/Θ as a function of the inhibitor concentration is linear.

atoms, such as oxygen, nitrogen and chlorine, in the functional groups. the free energy of adsorption (ΔG_{ads}) was calculated using the following Eq. (7):

$$K_{\text{ads}} = \frac{1}{55.55} e^{-\frac{\Delta G_{\text{ads}}}{RT}} \quad (7)$$

Where, R is the universal gas constant, and the absolute temperature is denoted by T . The molar concentration of water is expressed in mol/L and in solution its value is 55.5⁶².

Table 5. Thermodynamic parameters for adsorption of the inhibitors on steel at 298K.

Inhibitors	K_{ads} (L/mol)	ΔG_{ads} (KJ/mol)	R^2	Slopes
P1	$325,97 \cdot 10^3$	-41,4	0,99999	1,07348
P2	$819,39 \cdot 10^3$	-43,6	1	1,01815

Generally, values of ΔG_{ads} around or less than -20 kJ mol⁻¹ suggested that the adsorption process is related with the electrostatic interaction between charged

inhibitor molecules and the charged surface of the metal, which is termed as “physisorption”⁶³; while values around or higher than -40 kJ mol⁻¹ are

associated with sharing of charge or transfer from the inhibitor molecules to the metal surface to form a coordinate type of metal bond termed as “chemisorption”⁶⁴. In the present case of the adsorption of pyrazole derivatives, ΔG_{ads} was determined to be -41.4 kJ/mol of P1 and -43.6 kJ/mol of P2, suggesting the chemical adsorption of the inhibitor molecules into the corroding metal surface.

3.4. Temperature effect

Temperature is a key factor in inhibitor action. It can modify the metal-inhibitor interaction in the corrosive medium and inform the mode of adsorption of the

inhibitor. It is therefore vital to study the influence of these parameters on the action of pyrazole, which is an excellent inhibitor at 298K.

At this study, the inhibition efficiency of P1 and P2 on corrosion of stainless steel in H_2SO_4 2M without and with the addition of the inhibitor at a concentration of $10^{-3}M$ was carried at temperatures ranging between 298K and 328K. The polarization curves obtained are shown in Figure 6 and the electrochemical parameters derived from these curves are grouped in Table 6.

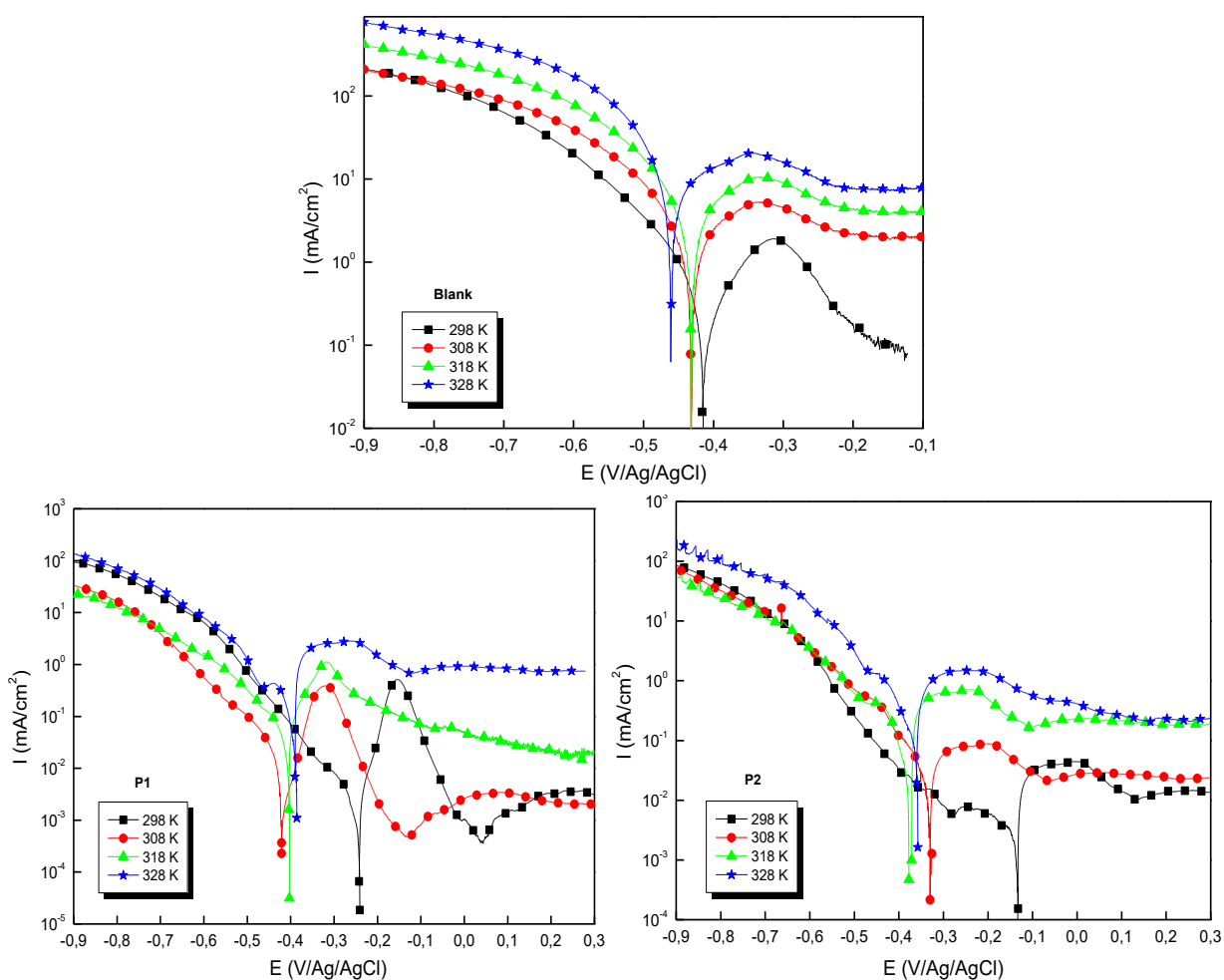


Figure 6. Representation of the cathodic and anodic polarization curves for stainless steel in H_2SO_4 2.0M without and with the addition of the inhibitor P1 and P2 at a concentration of $10^{-3}M$ with different temperatures

It is remarked that these curves exhibited the Tafel regions. It is also noted that the anodic and cathodic branches increased with increasing temperature. The curves in the cathodic part are parallel, indicating that the reduction of H^+ ions on the steel surface is done according to the same pure activation mechanism in all temperature range.

The data in Table 6 show clear that current densities increase with increasing temperature; hence a decrease in inhibitory efficiency for the two inhibitors has a concentration of $10^{-3} M$ in H_2SO_4 2.0 M medium. In addition, it can be noted that the inhibition efficiency decreases slightly in the presence of the inhibitors so that the two inhibitors remain effective against corrosion of the steel in sulfuric acid.

Table 6. Influence of temperature on the corrosion of steel/H₂SO₄ 2.0M Without and with the addition of P1et P2 of 10⁻³M and the corresponding inhibition efficiency.

Medium	T (K)	-E _{corr} (mV _{Ag/AgCl})	i _{corr} (μA/cm ²)	-β _c (mV/dec)	η _{pp} (%)
Blank	298	412	827	135	--
	308	432	1490	139	--
	318	429	2409	142	--
	328	460	3250	153	--
P1	298	248	57,5	110	93,0
	308	417	132,5	130	91,1
	318	400	265,4	125	88,9
	328	383	438,7	119	86,5
P2	298	133	13,0	124	98,4
	308	327	52,0	130	96,5
	318	376	132,0	136	94,5
	328	354	248,0	119	92,3

3.5. Thermodynamic parameters for activation

The variation in the logarithm of the corrosion rate as a function of the inverse of the absolute temperature (1000/T) is recorded in Figure 7. The curves obtained in the form of straight lines comply with Arrhenius' law (8).

$$i_{corr} = K \exp\left(-\frac{E_a}{RT}\right) \quad (8)$$

Where E_a is the activation energy, R is the perfect gas constant, k is a pre-exponential factor, T the absolute temperature and i_{corr} is the corrosion current density.

An alternative formula of the equation of Arrhenius allows the determination of the values of enthalpy ΔH_a and entropy ΔS_a, according to the following equation (9) ⁶⁵:

$$i_{corr} = \frac{RT}{Nh} \exp\left(\frac{\Delta S_a}{R}\right) \exp\left(-\frac{\Delta H_a}{RT}\right) \quad (9)$$

Where h: Planck Constant, N: Avogadro number, ΔH_a: Activation Enthalpy and ΔS_a: Activation Entropy.

The variation of ln(i_{corr}/T) as a function of the reciprocal of temperature is a line (Figure 5), with a slope equal to (-ΔH_a/R) and an intercept of (ln R/Nh + ΔS_a/R).

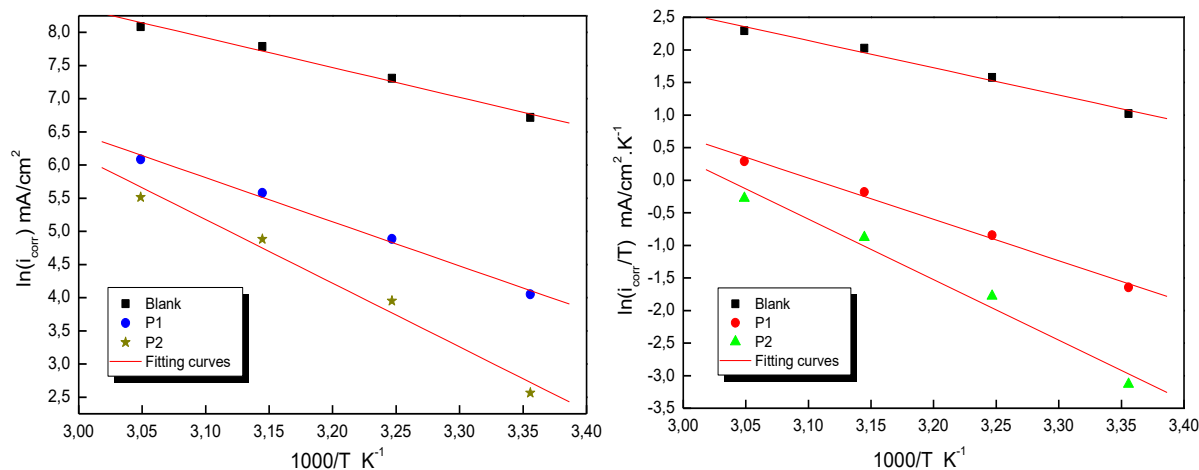


Figure 5. Arrhenius lines for stainless steel in H₂SO₄ 2.0M medium without and with the addition of the compounds P1 and P2 10⁻³M

The activation parameters (ΔH_a, ΔS_a and E_a) calculated from the slopes of the Arrhenius lines in

the absence and in the presence of the inhibitors P1 and P2 are grouped in Table 7.

Table 7. Thermodynamic parameters for corrosion of stainless steel without and with the addition of the inhibitors P1 and P2.

Medium	Compounds	Ea (KJ/mol)	ΔH_a (KJ/mol)	ΔS_a (J/mol.K)
H ₂ SO ₄ 2.0 M	Blank	37,4	34,8	-71,8
	P1	55,3	52,7	-33,8
	P2	79,8	76,3	36,8

From the [Table 7](#) it is clear that the Ea values of the solution containing P1 and P2 is higher than that in case of uninhibited solution which may be attributed to the formation of compact barrier film on the stainless-steel surface⁶⁶. The higher energy barrier for corrosion process in case of inhibited solutions suggests that adsorbed inhibitor's film prevents the charge/mass transfer reaction occurring on the surface^{67,68} and thus protecting metal from dissolution. The positive signs of the enthalpies ΔH_a reflected the endothermic nature of the steel dissolution process^{69,70}.

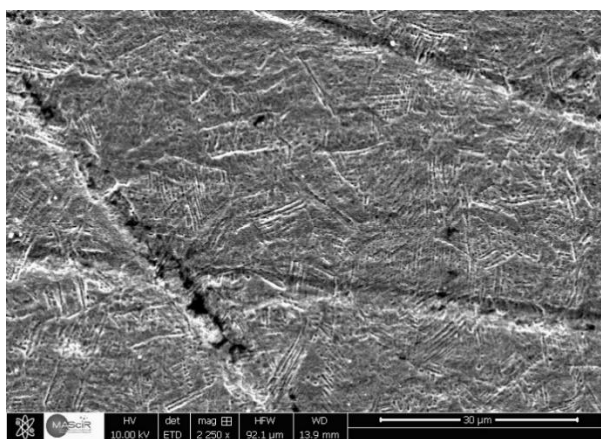
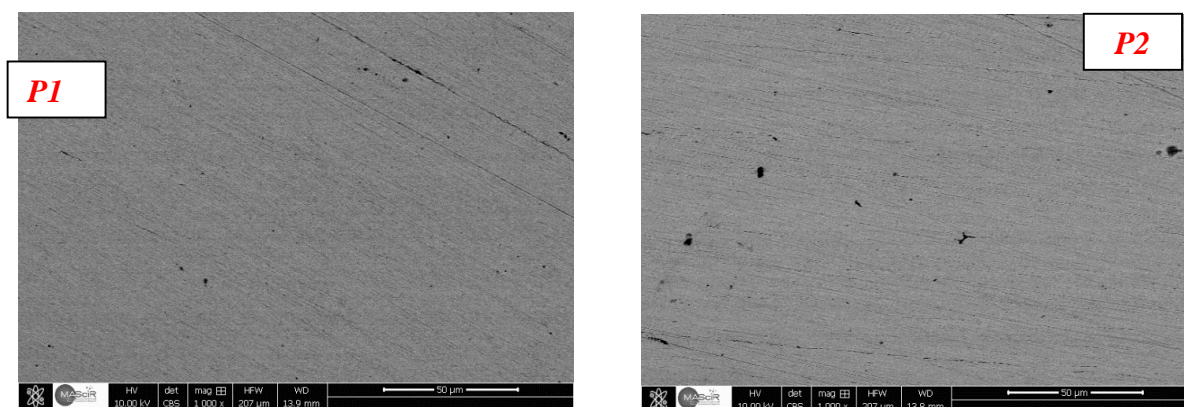
Meanwhile the values of activation entropies (ΔS_a) increase and negative in the presence of both inhibitors P1 meaning that a decrease in the disorder during the transformation of the reagents into

activated complex^{71,72}, in the case of P2 the value of ΔS_a high and positive meaning an increase in the disorder⁷³.

3.6. Surface analysis by SEM -EDX

SEM images of the sample after immersion in H₂SO₄ 2.0M for 6 hours at 298 K in the absence of inhibitor are shown in [Figure 6](#).

It is noted that the surface of the steel after immersion in H₂SO₄ 2.0M is severely damaged with the formation of several pits randomly distributed on the surface. This clearly shows that the steel undergoes almost generalized corrosion over the entire surface in the absence of the inhibitor. The grey areas correspond to iron oxide films.

**Figure 6.** SEM images of the steel surface after immersion in the H₂SO₄ 2.0M medium for 6 hours at 298**Figure 7.** SEM images of the steel surface after immersion in the H₂SO₄ 2.0M medium for 6 hours at 298 K in the presence of 10⁻³ P1 and P2

In the presence of 10⁻³ M of the compounds P1 and P2 in the H₂SO₄ 2.0M solution, [Figure 7](#) shows a

smoother, more homogeneous and brighter surface. By comparison with the image obtained

without inhibitor, we can conclude that the surface of the steel is almost free of corrosion. This is due to the formation of the adsorbed layers of the inhibitor on the steel surface. These results confirm the ability of products P1 and P2 to protect stainless steel and delay its corrosion in H_2SO_4 solutions by limiting electrolyte access to the surface.

An EDX analysis (Figure 8) was performed to identify the composition of the steel surface after immersion in H_2SO_4 2.0M in the absence and the presence of P1 and P2.

The presence of the oxygen peak in the EDX spectrum in Figure 8 clearly shows the formation of iron oxide from the corrosion of steel in H_2SO_4 medium.

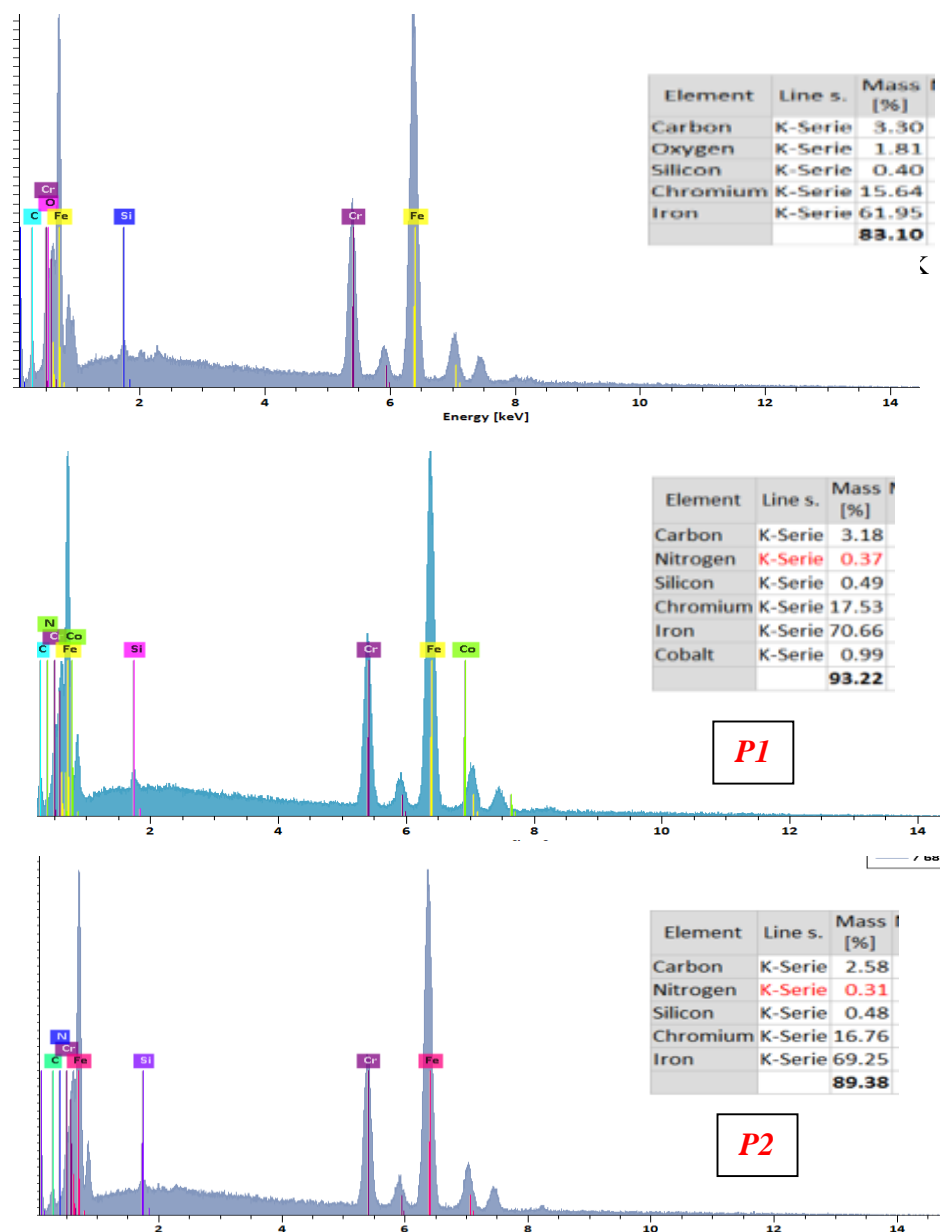


Fig. 9 EDX spectrum of the steel surface after immersion in a solution containing H_2SO_4 2.0M + 10^{-3}M of the inhibitors P1 and P2 at 298 K

The comparison of the two spectra in Figure 9 with the EDX spectrum of the corroded steel in H_2SO_4 2.0M (Figure 8), shows the absence of the oxygen peak and the presence of a nitrogen peak on the EDX spectra of both compounds. These observations confirm that these inhibitors used appear to prevent corrosion of the steel by forming a layer that limits the access of the electrolyte to the steel surface.

4. Conclusion

Concluding the experimental part, it was demonstrated that all techniques used, can characterize and to follow the corrosion inhibition process promoted by two pyrazole compounds: P1 and P2 was investigated. P1 and P2 exhibited excellent inhibition properties for stainless steel corrosion in H_2SO_4 2.0M solution, and their inhibitory efficiency increases with increasing concentration.

The obtained results showed that P1 and P2 acted as anodic type inhibitors of stainless-steel corrosion in H₂SO₄ 2.0M. Electrochemical impedance spectroscopy (EIS) measurement results indicated that the polarization resistance of the stainless steel increased with inhibitor concentrations to reach a maximum at 10⁻³M of P1 and P2 but P2 showed higher protection and performances than P1. This may be due to the presence of chloride atom, which improves adsorption of P2 on a charged metal surface. The adsorption characteristics of P1 and P2 followed the isothermal adsorption model of Langmuir. The study of temperature effect on the inhibition efficiency shows that this one decreases with the temperature increase. Which confirms that the adsorption of both pyrazole compounds is made by intermediate adsorption between physisorption and chemisorptions. Surface morphology studies confirmed the mitigation of stainless-steel corrosion by the formation of a protective film on the surface of the steel.

References

1. E. M. Jallouli, M. Fikrat, Colloque international sur les aciers inoxydables, Mons, **1988**, 18, 1.
2. E. M. Jallouli, 2ème Colloque Européen Corrosion dans les usines chimiques et para chimiques, Grenoble, **1994**, 2, 9-1.
3. M. A. Hajji, E. M. Jallouli, S. Belcadi, F. E. White, 3ème Colloque Européen sur la corrosion des industries chimiques et para chimiques, Lyon, France, **1997**.
4. F. M. El-Hossary, N. Z. Negm, S. M. Khalil, A. M. Abed El-Rahman, M. Raaif, S. Mändl, Effect of annealing temperature on hardness, thickness and phase structure of carbonitrided 304 stainless steel, *Appl. Phys. A.*, **2010**, 99, 489–495.
5. V. de F. C. Lins, G. A. dos S. Gonçalves, T. P. Leão, R. B. Soares, C. G. F. Costa, A. K. do N. Viana, Corrosion resistance of AISI 304 and 444 stainless steel pipes in sanitizing solutions of clean-in-place process, *Mater. Res.*, **2016**, 19, 333–338.
6. M. Finšgar, J. Jackson, Application of corrosion inhibitors for steels in acidic media for the oil and gas industry: A review, *Corros. Sci.*, **2014**, 86, 17–41.
7. A.-R. Grayeli-Korpi, H. Savaloni, M. Habibi, Corrosion inhibition of stainless-steel type AISI 304 by Mn coating and subsequent annealing with the flow of nitrogen at different temperatures, *Appl. Surf. Sci.*, **2013**, 276, 269–275.
8. M. Shabani-Nooshabadi, M. S. Ghandchi, Introducing the Santolinachamaecyparissus Extract as a Suitable Green Inhibitor for 304 Stainless Steel Corrosion in Strong Acidic Medium, *Metall. Mater. Trans. A.*, **2015**, 46, 5139–5148.
9. N. A. Negm, A. M. A. Sabagh, M. A. Migahed, H. M. A. Bary, H. M. E. Din, Effectiveness of some diquatery ammonium surfactants as corrosion inhibitors for carbon steel in 0.5M HCl solution, *Corros. Sci.*, **2010**, 52, 2122–2132.
10. S. M. Tawfik, Corrosion inhibition efficiency and adsorption behavior of N,N-dimethyl-4-(((1-methyl-2-phenyl-2,3-dihydro-1H-pyrazol-4-yl)imino)methyl)-Nalkylbenzenaminium bromide surfactant at carbon steel/hydrochloric acid interface, *J. Mol. Liq.*, **2015**, 207, 185–194.
11. M. Abdallah, H.M. Eltass, M. A. Hegazy, H. Ahmed, Adsorption and inhibition effect of novel cationic surfactant for pipelines carbon steel in acidic solution, *Prot. Met. Phys. Chem. Surf.*, **2016**, 52, 721–730.
12. J. Gasiorek, A. Szczurek, B. Babiarczuk, J. Kaleta, W. Jonesn, J. Krzak, Functionalizable Sol-Gel Silica Coatings for Corrosion Mitigation, *Materials*, **2018**, 11, 197.
13. Abass A. Olajire, Recent advances on organic coating system technologies for corrosion protection of offshore metallic structures, *Journal of Molecular Liquids*, **2018**, 269, 572–606.
14. E. McCafferty, Societal Aspects of Corrosion. In: Introduction to Corrosion Science, Springer, **2010**, 357.
15. W. Kautek, The galvanic corrosion of steel coatings: aluminum in comparison to cadmium and zinc, *Corros. Sci.*, **1988**, 28, 173-199.
16. M. Abdullah Dar, A review: plant extracts and oils as corrosion inhibitors in aggressive media. *Ind Lubr Tribol.*, **2011**, 63, 227.
17. K. Tebhji, B. Hammouti, H. Oudda, A. Ramdani, A. Benkadour, The inhibitive effect of bipyrazolic derivatives on the corrosion of steel in hydrochloric acid solution, *Appl. Surf. Sci.*, **2005**, 252, 1378-1385.
18. H. Tian, W. Li, K. Cao, B. Hou, Potent inhibition of copper corrosion in neutral chloride media by novel non-toxic thiadiazole derivatives, *Corrosion Science*, **2013**, 73, 281–291.
19. E.M. Sherif, S.-M. Park, Effects of 2-amino-5-ethylthio-1,3,4-thiadiazole on copper corrosion as a corrosion inhibitor in aerated acidic pickling solutions, *Electrochim. Acta*, **2006**, 51, 6556.
20. L. Ying, F. Haitao, Z. Yifan, W. Wuji, Study on the inhibiting behavior of AMT on bronze in 5% citric acid solution, *J. Mater. Sci.*, **2003**, 38, 407-411.
21. O. Blajiev, A. Hubin, Inhibition of copper corrosion in chloride solutions by amino-mercapto-thiadiazol and methyl-mercapto-thiadiazol: an impedance spectroscopy and a quantum-chemical investigation, *Electrochim. Acta.*, **2004**, 49, 2761-2770.
22. Z. Moradi, M. M. Attar, An investigation on the inhibitory action of benzazole derivatives as a consequence of sulfur atom induction, *Appl. Surf. Sci.*, **2014**, 317, 657–665.
23. S. S. Shivakumar, K. N. Mohana, Cantellaasiatica extracts as green corrosion inhibitors for mild steel in 0.5 M H₂SO₄, *Adv. Appl. Sci. Res.*, **2012**, 3, 3097–3106.

24. A. Aouniti, B. Hammouti, S. Kertit, M. Brighli, The inhibitive effect of some pyridines towards the corrosion of iron in hydrochloric acid solution, *Bull. Electrochem.*, **1998**, 14, 193.
25. A. El-Ouafi, B. Hammouti, H. Oudda, S. Kertit, R. Touzani, A. Ramdani, New bipyrazole derivatives as effective inhibitors for the corrosion of mild steel in 1M HCl medium, *Anti-Corros. Meth. Mater.*, **2002**, 49, 199.
26. W. Li, Q. He, S. Zhang, et al, Some new triazole derivatives as inhibitors for mild steel corrosion in acidic medium, *J Appl Electrochem.*, **2008**, 38, 289.
27. Z. Tao, S. Zhang, W. Li, B. Hou, Corrosion inhibition of mild steel in acidic solution by some oxo-triazole derivatives, *Corrosion Science*, **2009**, 51, 2588–2595.
28. M. Rajendran, D. Devapiriam, DFT calculations for corrosion inhibition of copper by tetrazole derivatives, *Journal of Chemical and Pharmaceutical Research*, **2015**, 7(1), 763-773.
29. V. V. Dhayabaran, I. S. Lydia, J. P. Merlin, P. Srirenganayaki, Inhibition of corrosion of commercial mild steel in presence of tetrazole derivatives in acid medium, *Ionics*, **2004**, 10, 123-125.
30. M. Yadav, R. R. Sinha, T. K. Sarkar, N. Tiwari, Corrosion inhibition effect of pyrazole derivatives on mild steel in hydrochloric acid solution, *Journal of Adhesion Science and Technology*, **2015**, 29, 1690-1713.
31. R. S. Abdel Hameed, H. I. Al-Shafey, A. S. Abul Magd, H. A. Shehata, Pyrazole Derivatives as Corrosion Inhibitor for C- Steel in Hydrochloric Acid Medium, *J. Mater. Environ. Sci.* **2012**, 3(2), 294-305.
32. A. Ghanbari, M. M. Attar M. Mahdavian, Corrosion inhibition performance of three imidazole derivatives on mild steel in 1 M phosphoric acid, *Materials Chemistry and Physics*, **2010**, 124, 1205–1209.
33. M. Ouakki, M. Galai, M. Rbaa, A. S. Abousalem, B. Lakhri, E. H. Rifi, M. Cherkaoui, Quantum chemical and experimental evaluation of the inhibitory action of two imidazole derivatives on mild steel corrosion in sulphuric acid medium, *Heliyon*, **2019**, 5, e02759.
34. E. Lamera, S. Bouacida, H. Merazig, A. Chibani, M. Le Borgne, Z. Bouaziz, A. Bouraiou, DMAP as a new efficient catalyst for the one-pot synthesis of condensed phthalazines, *Zeitschrift Für Naturforschung B*, **2017**, 72(5), 361–368.
35. M. H. Gonzalez, Etude d'un traitement multifonctionnel vert pour la protection contre la corrosion de l'acier au carbone API 5L-X65 en milieu CO₂, **2011**.
36. W. B. Rossiter, F. J. Hamilton, Physical methods of chemistry, Electrochemical methods, New-York: John Wiley & sons, Inc, **1986**, 2, 904.
37. I. Epelboin, C. Gabrielli, M. Keddam, H. Takenouti, Electrochemical Corrosion testing, *ASTM STP*, **1981**, 727.
38. M. Sahin, G. Gece, S. ilgic, Experimental and theoretical study of the effect of some heterocyclic compounds on the corrosion of low carbon steel in 3.5% NaCl medium, *Appl. Electrochem.*, **2008**, 38, 809-815.
39. M. Ouakki, M. Rbaa, M. Galai, B. Lakhri, E. H. Rifi, M. Cherkaoui, Experimental and Quantum Chemical Investigation of Imidazole Derivatives as Corrosion Inhibitors on Mild Steel in 1.0 M Hydrochloric Acid, *Journal of Bio-and Tribo-Corrosion*, **2018**, 4, 35.
40. A. B. Da Silva, E. D'Elia, J.A. da Cunha Ponciano Gomes, Carbon steel corrosion inhibition in hydrochloric acid solution using a reduced Schiff base of ethylenediamine, *Corros. Sci.* **2010**, 52, 788.
41. N. P. Zhuk, Course on Corrosion and Metal Protection, Metallurgy, Moscow, **1976**.
42. D. Ben Hmamou, R. Salghi, A. Zarrouk, H. Zarrok, O. Benali, M. Errami, B. Hammouti, Inhibition effect of horehound (*Marrubium vulgare* L.) extract towards C38 steel corrosion in HCl solution, *Res ChemIntermed.*, **2012**, 39(7), 3291-3302.
43. M. Rbaa, M. Galai, Y. El Kacimi, M. Ouakki, R. Touir, B. Lakhri, M. Ebn Touhami, Adsorption Properties and Inhibition of Carbon Steel Corrosion in a Hydrochloric Solution by 2-(4, 5-diphenyl-4, 5-dihydro-1h-imidazol-2-yl)-5-methoxyphenol, *Portugaliae Electrochimica Acta*, **2017**, 35(6), 323-338.
44. E. Ech-chihbi, M. E. Belghiti, R. Salim, H. Oudda, M. Taleb, N. Benchat, B. Hammouti, F. El-Hajjaji, Experimental and computational studies on the inhibition performance of the organic compound "2-phenylimidazo [1, 2-a] pyrimidine-3-carbaldehyde" against the corrosion of carbon steel in 1.0 M HCl solution, *Journal Surfaces and Interfaces*, **2017**, 9, 206–217.
45. A. O. Yüce, G. Kardaş, Adsorption and inhibition effect of 2-thiohydantoin on mild steel corrosion in 0.1 M HCl, *Corros. Sci.*, **2012**, 58, 86–94.
46. S. S. A. Rehim, H. H. Hassan, M. A. Amin, Corrosion and corrosion inhibition of Al and some alloys in sulphate solutions containing halide ions investigated by an impedance technique, *Appl. Surf. Sci.* **2002**, 189, 279.
47. R. Parsons, The electrical variable and the form of the isotherm for the adsorption of organic compounds at electrodes. *J. Electroanal. Chem.*, **1964**, 8, 93-98.
48. M. Ouakki, M. Galai, M. Cherkaoui, E. H. Rifi, Z. Hatim, Inorganic compound (apatite doped by Mg and Na) as a corrosion inhibitor for mild steel in phosphoric acidic medium, *Anal. Bioanal. Electrochem.*, **2018**, 10(7), 943-960.
49. X. Wu, S. Ma, S. Chen, Z. Xu, A. Sui, General equivalent circuits for faradaic electrode processes under electrochemical reaction control, *J. Electrochem. Soc.*, **1999**, 146, 1847.
50. L. Kadiri, M. Galai, M. Ouakki, Y. Essaadaoui, A. Ouass, M. Cherkaoui, E. H. Rifi, A. Lebki,

- Coriandrum Sativum. L Seeds Extract as a Novel Green Corrosion Inhibitor for Mild Steel in 1.0 M Hydrochloric and 0.5 M Sulfuric Solutions. *Anal. Bioanal. Electrochem.*, **2018**, 10, 249-268.
51. N. M'hanni, M. Galai, T. Anik, M. EbnTouhami, E. H. Rifi, Z. Asfari, R. Touir, Influence of additives selected calix [4] arenes on electroless copper plating using hypophosphite as reducing agent, *Surface Coatings Technol*, **2017**, 310, 8-16.
52. K. Rahmouni, M. Keddami, A. Srhiri, H. Takenouti, Corrosion of copper in 3% NaCl solution polluted by sulphide ions, *Corros. Sci.*, **2005**, 47, 3249-3266.
53. G. Kardas, The inhibition effect of 2-thiobarbituric acid on the corrosion performance of mild steel in HCl solutions, *J. Materials Science*, **2005**, 41, 337-343.
54. M. Behpour, S. M. Ghoreishi, N. Soltani, M. Salavati-Niasari, M. Hamadani, A. Gandomi, Electrochemical and theoretical investigation on the corrosion inhibition of mild steel by thiosalicylaldehyde derivatives in hydrochloric acid solution, *Corros. Sci.*, **2008**, 50, 2172-2181.
55. A. K. Singh, M. A. Quraishi, Effect of 2, 2' benzothiazolyl disulfide on the corrosion of mild steel in acid media, *Corros. Sci.*, **2009**, 51, 2752-2760.
56. J. Aljourani, K. Raeissi, M. A. Golzar, Benzimidazole and its derivatives as corrosion inhibitors for mild steel in 1M HCl solution, *Corros. Sci.*, **2009**, 51, 1836-1843.
57. C. H. Hsu, F. Mansfeld, Concerning the conversion of the constant phase element parameter Y0 into a capacitance, *Corrosion*, **2001**, 57, 747-748.
58. M. El Faydy, M. Galai, M. Rbaa, M. Ouakki, B. Lakhri, M. Ebn Touhami, Y. El Kacimi, Synthesis and application of new quinoline as hydrochloric acid corrosion inhibitor of carbon steel, *Anal. Bioanal. Electrochem.*, **2018**, 10(7), 815-839.
59. H. Tian, W. Hou, B. Li., Novel application of a hormone biosynthetic inhibitor for the corrosion resistance enhancement of copper in synthetic seawater, *Corros. Sci.*, **2011**, 53, 3435-3445.
60. P. Roy, P. Karfa, U. Adhikari, D. Sukul, Corrosion inhibition of mild steel in acidic medium by polyacrylamide grafted Guar gum with various grafting percentage: Effect of intramolecular synergism, *Corros. Sci.*, **2014**, 88, 246-253.
61. E. Kalman, B. Varhegyi, I. Bako, I. Felhosi, F. H. Karman, A. Shaban, Corrosion inhibition by 1-Hydroxy-ethane-1, 1-diphosphonic acid an electrochemical impedance spectroscopy study, *J. Electrochem. Soc.*, **1994**, 141, 3357-3360.
62. J. Flis, T. Zakroczyński, Impedance study of reinforcing steel in simulated pore solution with tannin, *J. Electrochem. Soc.* **1996**, 143, 2458.
63. F. M. Donahue, K. Nobe, Theory of organic corrosion inhibitors: adsorption and linear free energy relationships, *J. Electrochem. Soc.*, **1965**, 112, 886.
64. E. Kamis, F. Bellucci, R. M. Latanision, E. S. H. El-Ashry, Acid corrosion inhibition of nickel by 2-(triphenylphosphoranylidene) succinic anhydride, *Corrosion*, **1991**, 47, 677-686.
65. M. Yadav, L. Gope, N. Kumari, P. Yadav, Corrosion inhibition performance of pyranopyrazole derivatives for mild steel in HCl solution: Gravimetric, electrochemical and DFT studies, *J. Mol. Liq.*, **2016**, 216, 78-86.
66. S. M. Shaban, A. A. Abd-Elaal, S. M. Tawfik, Gravimetric and electrochemical evaluation of three nonionic dithiol surfactants as corrosion inhibitors for mild steel in 1 M HCl solution, *Journal of Molecular Liquids*, **2016**, 216, 392-400.
67. L.C. Murulana, M.M. Kabanda, E.E. Ebenso, Investigation of the adsorption characteristics of some selected sulphonamide derivatives as corrosion inhibitors at mild steel/hydrochloric acid interface: Experimental, quantum chemical and QSAR studies, *Journal of Molecular Liquids*, **2016**, 215, 763-779.
68. Y. Essaadaoui, M. Galai, M. Ouakki, L. Kadiri, A. Ouass, M. Cherkaoui, E. H. Rifi, A. Lebkiri. Study of the Anticorrosive Action of Eucalyptus Camaldulensis Extract in case of Mild Steel in 1.0 M HCl, *Journal of Chemical Technology and Metallurgy*, **2019**, 54(2), 431-442.
69. O. Fergachi, F. Benhiba, M. Rbaa, M. Ouakki, M. Galai, R. Touir, B. Lakhri, H. Oudda, M. Ebn Touhami, Corrosion inhibition of ordinary steel in 5.0 M HCl medium by benzimidazole derivatives: electrochemical, UV-visible spectrometry, and DFT calculations, *Journal of Bio-and Tribo-Corrosion*, **2019**, 5, 21.
70. K. Tarfaoui, M. Ouakki, M. Galai, M. Nehiri, M. Ebn Touhami, N. Barhada, M. Ouhssine, Valorization of the essential oil of Zingiber officinale by its Use as inhibitor against the corrosion of the carbon steel in acid medium hydrochloric acid 1M, *Mediterranean Journal of Chemistry*, **2019**, 8(1), 17-24.
71. M. Yadav, S. Kumar, N. Tiwari, I. Bahadur, E. E. Ebenso, Experimental and quantum chemical studies of synthesized triazine derivatives as an efficient corrosion inhibitor for N80 steel in acidic medium, *J Mol Liq.*, **2015**, 212, 151-67.
72. S. Martinez, I. Stern, Thermodynamic characterization of metal dissolution and inhibitor adsorption processes in the low carbon steel/mimosa tannin/sulfuric acid system, *Appl. Surf. Sci.*, **2002**, 199, 83-89.
73. M. Elachouri, M. S. Hajji, M. Salem, S. Kertit, J. Aride, R. Coudert, E. Essassi, Some nonionic surfactants as inhibitors of the corrosion of iron in acid chloride solutions, *Corros.*, **1996**, 52, 103-108.